INTRODUCTION

Parkinson's disease (PD) results primarily from the death of dopaminergic neurons in the substantia nigra and aggregated deposits termed Lewy bodies in the brain. The major component of these intracellular deposits is aggregated α-synuclein (α-syn), a 140-amino acid protein that is abundantly expressed in presynaptic terminals (Reynolds, Soragni et al. 2011; Vekrellis, Xilouri et al. 2011; Hansen and Li 2012). α-Syn accumulation is known to be an early step in the pathogenesis of both sporadic and inherited PD, but the molecular mechanism of how α-syn is accumulated in the intracellular deposits of Lewy bodies remains unclear (Windisch, Wolf et al. 2008).

Recent evidence suggests that overexpressed and/or misfolded α-syn can be released into the extracellular space by unconventional exocytosis or via exosomes and transit to other cells (Lee, Patel et al. 2005; Emmanouilidou, Melachroinou et al. 2010; Jang, Lee et al. 2010). Indeed, secreted α-syn is readily detected in the plasma and CSF of humans and in the culture media of neuronal cells (El-Agnaf, Salem et al. 2003). The cell-to-cell transfer of secreted α-syn consequently leads to an accumulation of intracellular α-syn and precedes the misfolding of small aggregates in the recipient cells (Desplats, Lee et al. 2009; Hansen, Angot et al. 2011; Volpicelli-Daley, Luk

et al. 2011).

Membrane trafficking plays a central role in the maintenance of cell organization and organelle homeostasis, and for intercellular communication (Cheung and de Vries 2008; Varkey, Isas et al. 2010). Transferrin (Tfn)-mediated iron uptake has been extensively studied as an example of intracellular trafficking. Upon binding of diferric transferrin (Fe_2Tf) to transferrin receptor (TfR), it transports iron into cells through receptor-mediated endocytosis. The internalized iron is released from early endosomes into the cytoplasm within an acidic environment, whereas Tfn and TfR recycle back to the cell surface at a neutral pH. Due to this unique characteristic, TfR is used as an indicator for membrane trafficking pathways recycling between endosomes and the plasma membrane (Ullrich, Reinsch et al. 1996; Matsui, Itoh et al. 2011).

A recent study showed that the overexpression of wild-type α-syn and polyunsaturated fatty acids (PUFAs) increased vesicle endocytosis and recycling in both neuronal and non-neuronal cells (Ben Gedalya, Loeb et al. 2009), but there is still debate on whether secreted α-syn has any effect on membrane trafficking in neighboring cells and if it does, then which particular species of α-syn would be responsible for that.

In the present study, we directly investigated the effects of secreted α-syn from differentiated SH-SY5Y cells on membrane trafficking by observing the uptake of transferrin, which is efficiently taken up into cells by the process of receptor-mediated endocytosis. We further investigated which forms of α-syn in aggregations are responsible for the effects of secreted α-syn uptake. Our finding provide a possible mechanism by which the secreted oligomeric form of α-syn may cause multiple defects in membrane trafficking when α-syn enter cells from extracellular space. Therefore, these finding may provide valuable insights into possible new therapeutic strategies and the development of suitable drug targets to inhibit oligomeric α-syn uptake in recipient cells which may lead to therapies to prevent or control PD (Brundin and Olsson 2011).

MATERIALS AND METHODS

Preparation of cell extract and conditioned medium (CM)

Differentiated SH-SY5Y cells were infected with adenoviral vector expressing either human α-synuclein (α-syn) or β-galactosidase (LacZ). Two days after infection, the growth media were replaced with the serum-free media. After 18 hours of incubation at 37℃, the conditioned media were collected and centrifuged at 1,000 × g for 10 min, and subsequently, at 10,000 × g for 10 min to remove cell debris and dead cells. The recovered supernatants were concentrated using 10,000 molecular weight cut-off filters (Millipore, Billerica, MA).

For extraction of cellular proteins, the cells were washed ice-cold phosphate-buffered saline (PBS) and harvested in the extraction buffer (PBS/1% Triton X-100/protease inhibitor cocktail). The extract was centrifuged at 16,000 × g for 10 min to obtain the Triton-soluble (supernatant) and –insoluble (pellet) fractions. The protein samples (10 μg) were loaded onto 12% SDS-PAGE. The primary antibody used for western analysis was monoclonal anti-α-synuclein antibody, syn-1 (BD Biosciences, San Jose, CA), and anti-β-galactosidase antibody (Developmental Studies Hybridoma Bank, Univ. of Iowa, Iowa City, IA).

Thioflavin T binding assay

40 μl of each sample was mixed with 10 μM thioflavin T solution in 10 μM glycine buffer (pH 8.5) and incubated at room temperature for 5 min. Absorbance was measured with excitation at 450 nm and emission at 490 nm with a SpectraMax GEMINI EM (Molecular Probes, Eugene, OR)

Circular dichroism (CD)

CD spectra of protein samples (0.5 mg/ml) were recorded from 190 to 260 nm with a step resolution of 1.0 nm, band width of 1.0 nm and an average time of 100 nm/min by using J-810 spectropolarimeter (Jasco, Mountain View, CA). For all spectra, an average out of 10 separates measurements was obtained.

Electron microscopy (EM)

Each sample was dropped on the formvard-coated grids and negatively stained with 1% (w/v) uranyl acetate. And then, samples were washed with distilled water. Electron microscopy images were obtained at 100 kV on a Philips CM electron microscope (Philips, Eindhoven, Netherlands)

Preparation of recombinant α-syn and aggregates

α-Syn expressed in *Escherichia coli* BL21 DE3 was purified using sequential column chromatography, including anion exchange (High-trap Q column, GE healthcare Life science, Pittsburgh, PA) and size exclusion column chromatography (Sephacryl S-200, GE healthcare Life science). Bacterial endotoxins were removed from recombinant α-syn using the Toxineraser endotoxin removal kit (Genscript, Piscotaway, NJ). Endotoxin levels were determined using the Toxinsensor chromogenic LAL endotoxin assay kit (Genscript) (< 0.015 endotoxin unit/1 mg of α-syn). For spontaneous oligomerization, lyophilized recombinant α-syn was dissolved in PBS (1 mg/ml) and incubated at 4℃. After two days of incubation, protein was filtrated using 100,000 molecular weight cut-off centrifugal filters (Millipore).

.

Cell culture/ Tfn uptake and recycling assay

For Tfn uptake, COS-7 cells were grown on coverslips in DMEM supplemented with 10% FBS and starved for 6 h in serum-free DMEM before treatment with CM or control medium for 2h. The cells were further incubated in serum-free DMEM with 20 mM HEPES containing 20 μg/ml Texas red Tfn (Molecular probe) for 3min, 5min and 10 min at 37℃, then washed with PBS, acid stripped (150 mM NaCl, 2 mM $CaCl_2$, and 25 mM CH_3COONa, pH 4.5) on ice and immediately fixed in 4% paraformaldehyde.

To study Tfn recycling after continuous uptake, cells were incubated at 37℃ in serum-free DMEM/HEPES containing 20 μg/ml Texas red Tfn for 60 min, then loaded with 100 μg/ml unlabeled Tfn (Sigma) and further incubated at 37℃ for various lengths of time. The cells were washed with ice-cold PBS, acid stripped on ice and fixed immediately. Images were taken on a Zeiss Axiovert microscope (Carl Zeiss, Jena, Germany) using a 60 X, 1.25 N.A. oil lens and Hamamatsu OrcaII CCD camera (Hamamatsu Photonics, Hamamatsu City, Japan). Texas red intensities were averaged over individual cells and analyzed using MetaMorph Imaging software (Universal Imaging Corp., West Chester, PA). Data are presented as means ± S.E. Statistical analyses were carried out with SPSS statistics 18 (IBM Corporation, Armonk, NY). For multiple conditions, we compared means by ANOVA followed by Turkey's HSD ***post hoc*** test.

Immunostaining of α-syn

COS-7 cells were starved for 6 h in serum-free DMEM and treated with CM in the presence or absence of 40 μM of DD-11 for 2h, and fixed. The cells were incubated at 4℃ in α-synuclein 274 antibody, which react only to human α-syn (1:500 in PBS/3% BSA) followed by incubation with the anti-Mouse Oregon green antibody (1:1000 in PBS/3% BSA, Molecular Probes)

for 45 min. Detailed procedures for production and characterization of this monoclonal human α-syn have been described previously (Lee, Bae et al. 2011; Bae, Lee et al. 2012).

Measurement of cell surface TfR/TIRF microscopy

Surface levels of TfR were determined in the presence of 50 μg/ml of cychloheximide (Sigma). COS-7cells were starved for 6 h and preincubated with 50 μg/ml of cychloheximide for 1h before the treatment of CM or control medium, which contained 50 μg/ml of cychloheximide in serum-free DMEM for 2 h. The cells were washed with ice-cold PBS and incubated in serum-free DMEM with 20 mM HEPES containing 20 μg/ml Texas red Tfn at 4℃ for 10 min. Unbound Tfn was removed by washing with PBS and fixed in 4% paraformaldehyde. For total internal reflection fluorescence (TIRF) microscopy, cells were imaged using an Olympus IX-71 microscope fitted with a 60X 1.45 N.A. TIRF lens and controlled by Cell^{M} software (Olympus, Tokyo, Japan). Laser line (488 nm diode laser) was coupled to the TIRFM condenser through an optical fiber. The calculated evanescent depth was ≈150 nm. Cells were typically imaged with 0.1- to 0.2 s exposures and detected with back-illuminated Andor iXon887 EMCCD camera (512 X 512, 16-bit; Andor Technologies, Belfast, UK). MetaMorph Imaging Software

was used for analysis.

Mathematical Analysis

Mathematical models of the experimental data were constructed as systems of ordinary differential equations (ODEs), corresponds to a distinguishable biological state of the TfR. This is because of Tfn follows a linear sequential reaction, which is internalized to the endosomal compartment from the TfR at the cell surface and recycles back to the plasma membrane with functions of time. The models were coded in MATLAB version 7.40 (MathWorks, Natick, MA) and solved using the ode45 functions.

The mathematical models for the TfR are as follows.

$$\frac{\mathrm{dTfRM1}}{\mathrm{dt}} = k3\mathrm{TfRM2} - k1\mathrm{TfRM1} \qquad \text{(Eq.1)}$$

$$\frac{\mathrm{dTfRE}}{\mathrm{dt}} = k1\mathrm{TfRM1} - k2\mathrm{TfRE} \qquad \text{(Eq.2)}$$

$$\frac{\mathrm{dTfRM2}}{\mathrm{dt}} = k2\mathrm{TfRE} - k3\mathrm{TfRM2} \qquad \text{(Eq.3)}$$

Where *k*1, *k*2, *k*3 are the rate constants for each condition and TfRM1, TfRE and TfRM2 are the arbitrary units of TfR at the plasma membrane, the TfR in the endosomal compartments when it is internalized and the TfR at the plasma membrane once it's recycled respectively. (See "Results" for a description of receptor states)

RESULTS

Secreted α-syn is taken up by dynamin-dependent endocytosis

Secreted α-syn in conditioned medium (CM) was obtained from differentiated SH-SY5Y cells, infected with an adenoviral vector expressing either human α-syn or β-galactosidase (LacZ) (**Fig. 7**). To test whether this secreted α-syn enters cells by dynamin-dependent endocytosis, we performed an immunofluorescence staining of α-syn in COS-7 cells with the endocytosis inhibitor of DD-11, a potent inhibitor of the GTPase activity of dynamin (Lee, Jung et al. 2010) (**Fig. 8**). COS-7 cells were starved for 6 hours in plain DMEM (no serum, antibiotics or nutrients). Cells were then treated with a mixture of secreted α-syn-containing medium in the presence or absence of 40 μM DD-11 for 2 hours at 37 ˚C. Fig. 1 clearly demonstrates that the secreted α-syn is taken up by dynamin-dependent endocytosis because DD-11 almost completely inhibits α-syn uptake into COS-7 cells (**Fig. 1A**).

Secreted α-syn enhances the rate of Tfn internalization.

To investigate a possible role of secreted α-syn in membrane trafficking, we performed a Tfn uptake assay by using Texas-red conjugated Tfn for the experiments (Kim, Park et al. 2010; Park, Kim et al. 2010). COS-7 cells were

grown on coverslips and starved for 6 hours in plain DMEM (no serum, antibiotics or nutrients). The secreted α-syn containing medium and a control medium were treated in COS-7 cells for 2 hours and incubated at 4 ˚C in serum-free DMEM/HEPES containing 20 ug/ml Texas red Tfn to allow binding of Tfn to its receptor before the internalization at 37 ˚C. Unbound Tfn was removed by washing with PBS and cells were transferred to 37 ˚C at different time points; 3 min, 5 min and 10 min to observe first round of endocytosis kinetics. The representative fluorescence images of Tfn endocytosis in COS-7 cells for the control (bottom panel) and α-syn(top panel) at each time point is shown (**Fig.2A**). The Tfn internalization was significantly increased with exogenous treatments of secreted α-syn (average texas red Tfn fluorescence in a.f.u: 3 min; 66.14±6.64, 5 min; 85.58± 10.01, 10 min; 110.42±12.56, **Fig.2B**) compared to the control groups (3 min ; 56.67±8.07, 5 min; 69.79±8.38, 10 min 87.54±9.36, **Fig.2B**) . The endocytic rates were calculated from a linear regression of each average fluorescence intensity with a slope of 6.065±0.208 for secreted α-syn-treated cells and 4.245±0.305 for the control, indicating that the secreted α-syn in CM transport the Tfn from the TfR at the cell surface to the sorting endosome much rapidly than the control and enhanced the rate of Tfn internalization (**Fig. 2B, C**).

Secreted α-syn enhances the rate of Tfn recycling

To test the effect of secreted α-syn in CM on Tfn recycling after internalization, COS-7 cells were loaded with 20 μg/ml of Texas red Tfn in serum-free DMEM/HEPES at 37℃ for 60 min to saturate the entire endocytic recycling pathway and 100 μg/ ml of unlabeled Tfn was subsequently added and incubated at 37℃ at indicated time, shown in **Fig. 3A** (Kim, Kim et al. 2006). The quantification of average intensity showed that secreted α-syn significantly enhanced the Tfn recycling compared to the control (τ =17.6 ±1.21 min for the control and τ =13.67±1.53 min for secreted α-syn- treated cells. **Fig. 3C)**.The initial average fluorescence intensity with the secreted α-syn at 0 min was significantly lower than that with control (494.73 ± 63.86 for the α-syn and 592.01 ± 58.41 for the control**, Fig. 3B**), suggesting less accumulation of Tfn in the endosomal compartment, which correlates well with faster Tfn recycling in cells with secreted α-syn.

Mathematical modeling of TfR trafficking estimates that secreted α-syn increases the levels of TfR at the cell surface

Based on our observed data from the TfR trafficking, we constructed a mathematical model of experimental data using a system of ordinary

differential equations to estimate the levels of TfR at the cell surface. The schematic diagram of our model is shown in **Fig. 4A**. We suggested that one cycle of the TfR trafficking occurs within 30 minutes and both the α-syn-treated cells and control cells initially have the same number of TfR at the cell surface. Each step of graphs was modeled using by exponential decay constants, where each decay constants are obtained by 1/ τ from Fig. 2B and 3C. The *k*1 was calculated from Fig. 2B values with an equation of A*(1-exp (-t/ τ), when we assume that y=0 at t=0. The A= 90.93 for control and A = 118.29 for α-syn-treated cells and each single exponential fitting has a R^2= 0.998 for control and R^2= 0.999 for α-syn-treated cells. The rate constants that we have used in our modeling were *k*1 = 0.202, *k*2 = 0.057 and *k*3 = 0.13 for control and *k*1= 0.31, *k*2= 0.073 and *k*3 = 0.077 for the α-syn-treated cells. Through this modeling, we were able to track the TfR in each condition (Fig. 4B and C for the control and α-syn, respectively). The results clearly demonstrated that α-syn treated cells would have higher surface levels of TfR than that of control (Fig. 4D).

Secreted α-syn increases the levels of cell surface TfR

To determine the TfR levels at the cell surface, we preincubated cells with 50 μg/ml of cychloheximide (CHX) for 2 h (Du, Zhang et al. 2011), which inhibits protein synthesis to eliminate possible complications caused by α-

syn effects on TfR synthesis, and the total internal reflection fluorescence microscopy (TIRFM) was used to selectively visualize the cell surface TfR for each condition(**Fig. 5A)**. The number of puncta/100 μm^2 of TfR at the cell surface in COS-7 cells treated with CM was increased approximately threefold compared to the control (the number of puncta/100 μm^2= 7.683 for the control and the number of puncta/100 μm^2= 22.103 for the α-syn, **Fig. 5B**) while the total level of TfR was not affected (**Fig. 5C**).

Soluble oligomeric secreted α-syn enhances Tfn internalization.

We next tested which species of α-syn in aggregations are responsible for the effects of secreted α-syn in CM. Since our CM was a mixture of the monomeric, oligomeric and fibrillar forms, it is uncertain which particular species of α-syn affected membrane trafficking in recipient cells. Thus, we prepared media containing recombinant α-syn in aggregations restricted to monomeric, fibrillar and oligomeric forms **(Fig. 10 and 11).** The result showed that there is no significant difference in the Tfn internalization for the monomeric or fibrillar forms compared to the control (**Fig. 6A** and **B**), suggesting that the soluble oligomeric form of α-syn in CM may be responsible for the effects of α-syn on membrane trafficking in recipient cells.

To further corroborate this, we next prepared a mixture of α-syn monomers

and oligomers (**Fig. 12**) and filtered to separate the monomers and oligomers in the mixture, which was then tested subsequently for effects on Tfn uptake. While filtered monomers (0.2 μM) failed to affect Tfn uptake, the oligomers (0.2 μM) of α-syn enhanced Tfn internalization compared to the control, indicating the role of the soluble oligomeric form of α-syn in Tfn internalization (**Fig. 6C** and **D)**

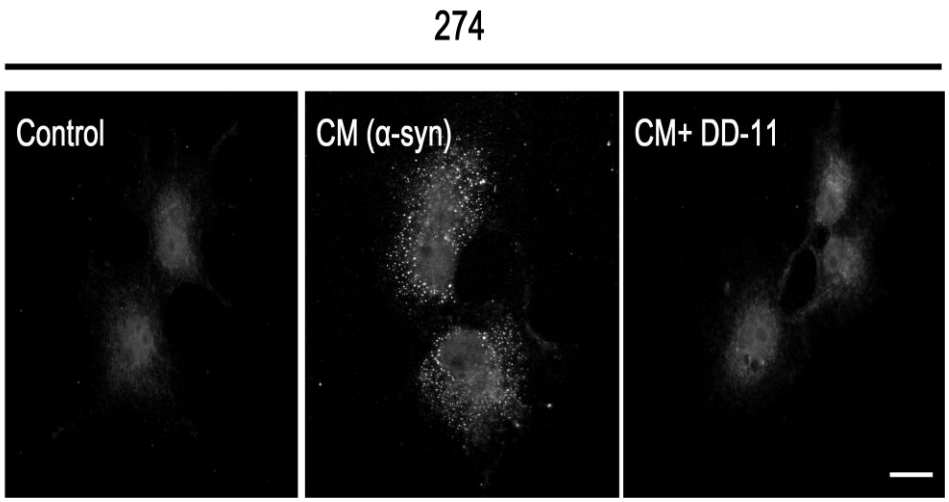

Figure 1. Secreted α-syn is transferred by dynamin-dependent endocytosis

(A) Immunocytochemistry with anti-α-syn 274 antibody performed on COS-7 cells, which were treated with control medium or CM in the absence or presence of 40 μM of DD-11 for 2 h at 37 ˚C. .

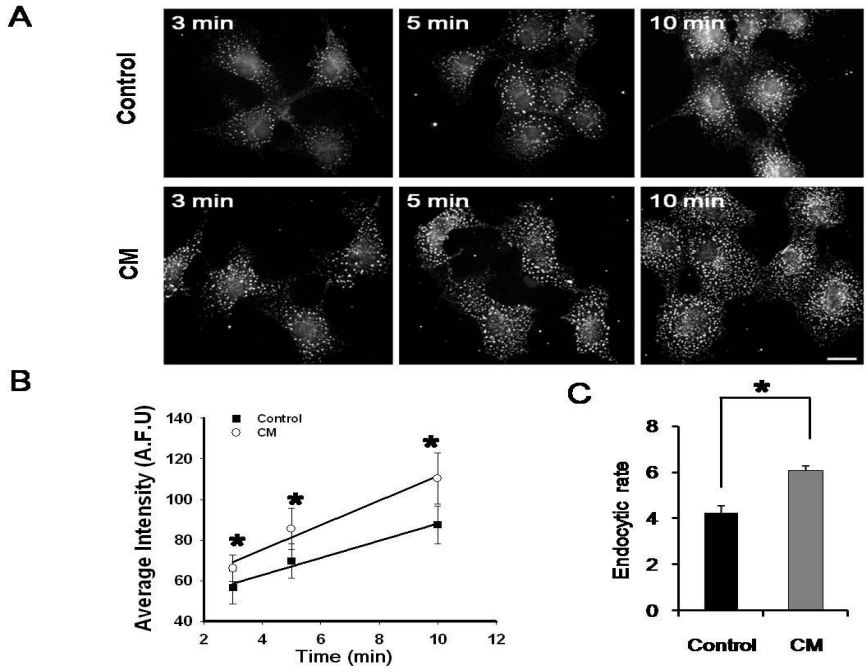

Figure 2. Secreted α-syn increases the rate of Tfn internalization

(A) Representative images of Tfn internalization for the control (top panel) and α-syn (bottom panel) with various time points in COS-7 cells. Single-round kinetics of Tfn uptake were determined for the indicated time. **(B)** Average fluorescence intensity was measured at each time point. Mean of 15 cells ± S.E. in each independent experiment were measured by selecting the region of interest to the cell area, n = 5, * $p < 0.05$, Student's *t*-test. Linear fitted graphs were obtained from each average fluorescence intensity. **(C)** Endocytic rate was measured by a linear regression of each average fluorescence intensity with a slope of 6.065±0.208 for α-syn and 4.245±0.305 for the control.

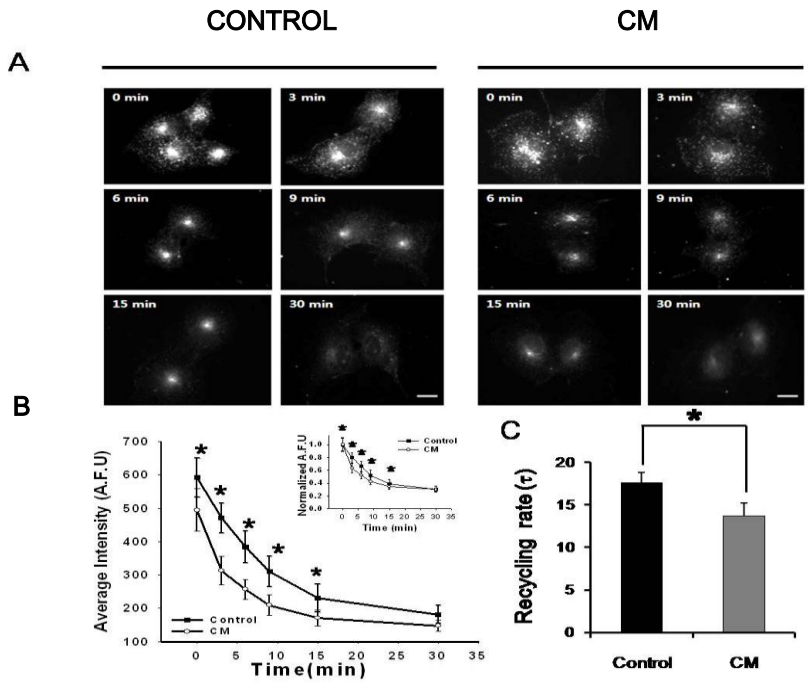

Figure 3. Secreted α-syn increases the rate of Tfn recycling

(A) Representative images of Tfn recycling for the control (left) and α-syn (right) in COS-7 cells. Recycling of Tfn from the endosome was measured at indicated time. **(B)** Average fluorescence intensity of Texas red was measured at each time point. Mean of 20 cells ± S.E. in each independent experiment were measured by selecting the region of interest to the cell area, n = 6,* $p < 0.05$, Student's *t*-test. The inset shows the normalized average fluorescence intensity graphs, fitted by a single exponential for each condition. **(C)** Recycling rate was fitted by a single exponential with τ =17.6 ±1.21 min for the control and τ =13.67±1.53 min for secreted α-syn- treated cells.

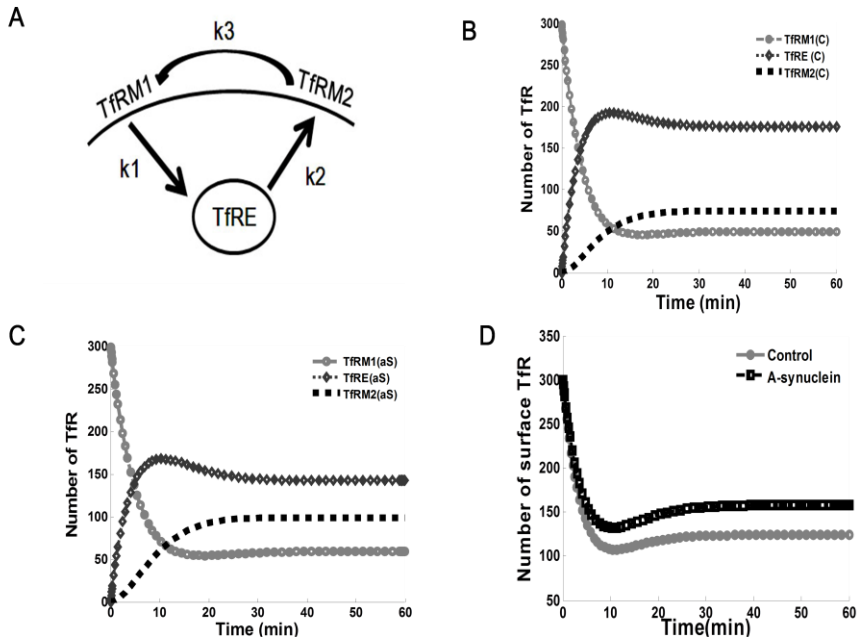

Figure 4. Mathematical modeling estimates the number of cell surface TfR.

(A) A schematic diagram of the TfR trafficking, where TfR is internalized from the cell surface and recycled back to the plasma membrane as functions of time. **(B, C)** The time course of TfR in each condition with rate constants *k*1, *k*2 and *k*3 for the control and α-syn-treated cells. TfRM1, TfR at the cell surface; TfRE, TfR in the endosomal compartment; TfRM2, TfR at the plasma membrane once it is recycled back to the cell surface. **(D)** The theoretical TfR surface occupancy (TfRM1+TfRM2) was solved over time.

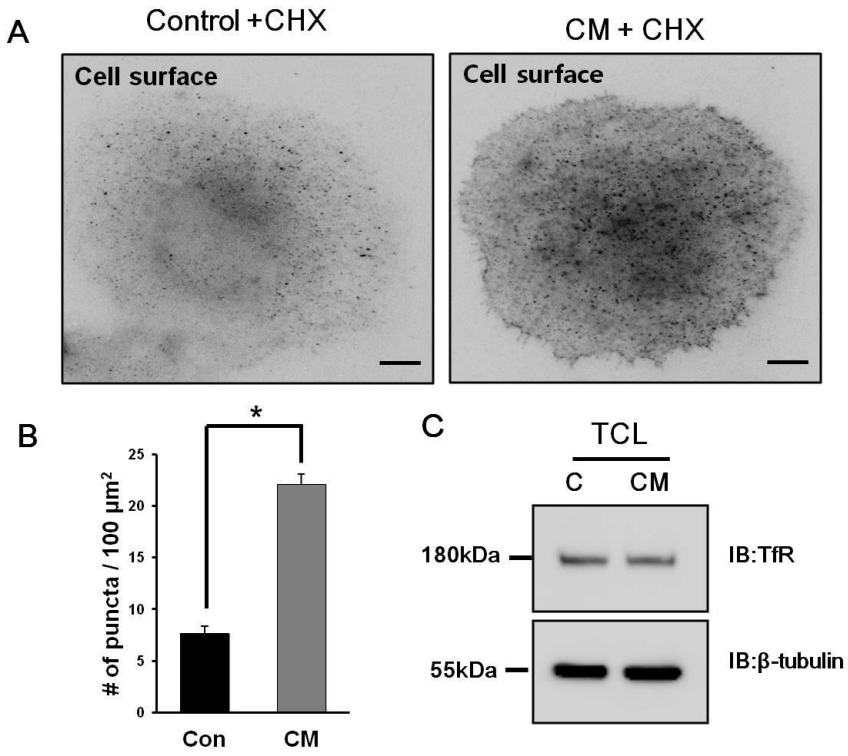

Figure 5. Secreted α-syn increases the levels of cell surface TfR

(A) Representative TIRF images of cell surface TfR levels for the control (left) and α-syn (right). The levels of cell surface TfR were measured by using cycloheximide. Scale bar = 20 μm. **(B)** The number of puncta per 100 μm^2 of the TfR in COS-7 was quantified, n =5,* $p< 0.01$, Student's *t*-test. **(C)** Cos-7 cells were serum-starved for 6 h and treated with CM or control medium for 2 h. Cell lysates were processed for SDS-PAGE and a western blot analysis was performed with anti-TfR antibody.

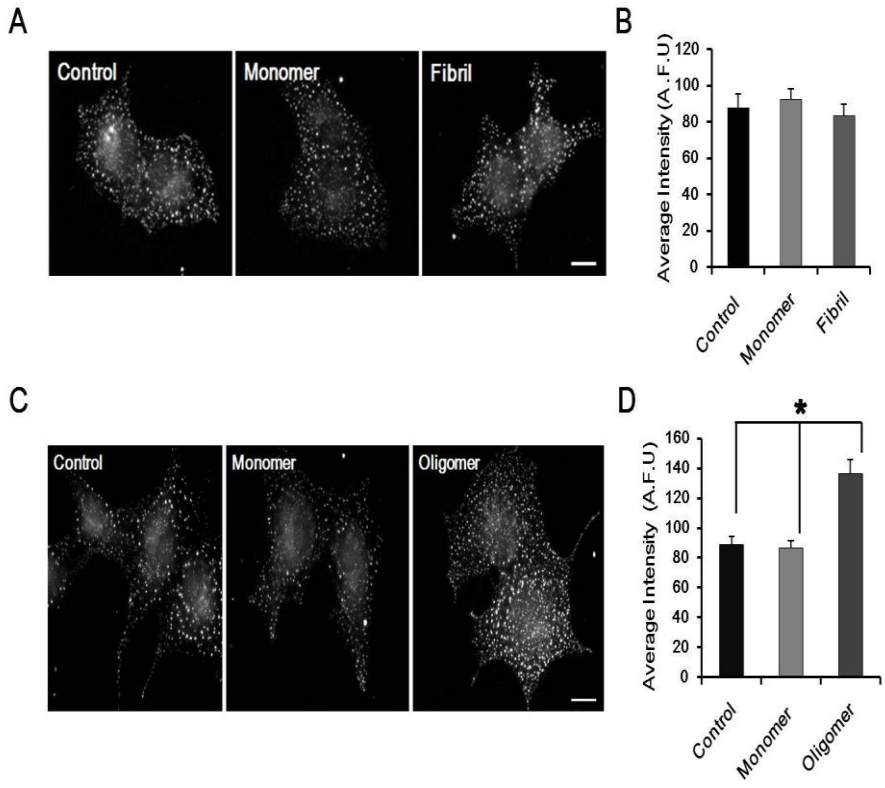

Figure 6. Soluble oligomer α-syn enhances the Tfn internalization.

(A) Representative images of each aggregation form are shown. Tfn uptake assay was carried out for 10 min at 37˚C with 0.2 μM of monomeric and fibrillar forms of α-syn. **(B)** Average fluorescence intensity was quantified for each condition, n= 5 * p< 0.05, Student's *t*-test. **(C)** Representative images of Tfn internalization for each aggregation form of α-syn: filtered monomer and oligomer with control medium. Scale bar = 20 μm. **(D)** Average fluorescence intensity was quantified for each condition, n = 10 one-way ANOVA followed by the Tukey's HSD *post hoc* test, *p< 0.05.

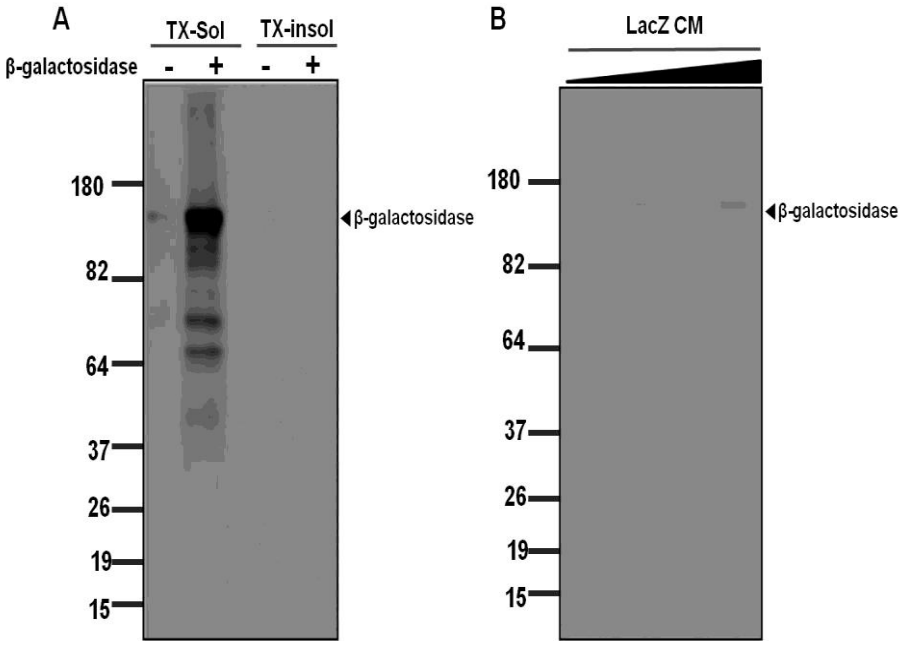

Figure 7. Western blot analysis of β-galactosidase (LacZ) in cell extracts and conditioned media (CM) (A) Western analysis of β-galactosidase in the extracts. The extracts were obtained from differentiated SH-SY5Y cells overexpresssing LacZ. Tx-s, Triton X-100-soluble; Tx-in, Triton X-100-insoluble**. (B)** Western analysis of LacZ. in the CM.

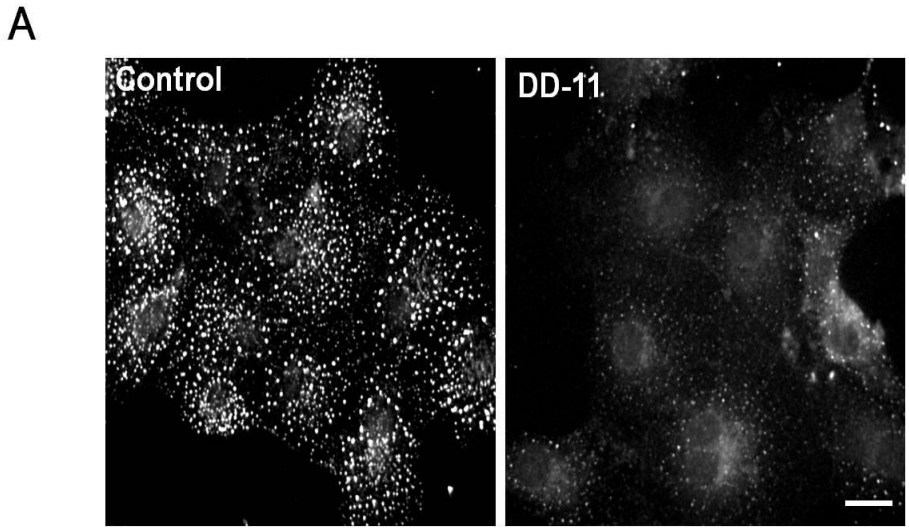

Figure 8. DD-11 inhibits the transferrin uptake (A) Representative image of Tfn uptake in the absence or presence of 40 μM DD-11 (Dynamin GTPase blocker). Tfn uptake assay was carried out for 10 min at 37˚C in the presence or absence of DD-11 and 0.1% DMSO.

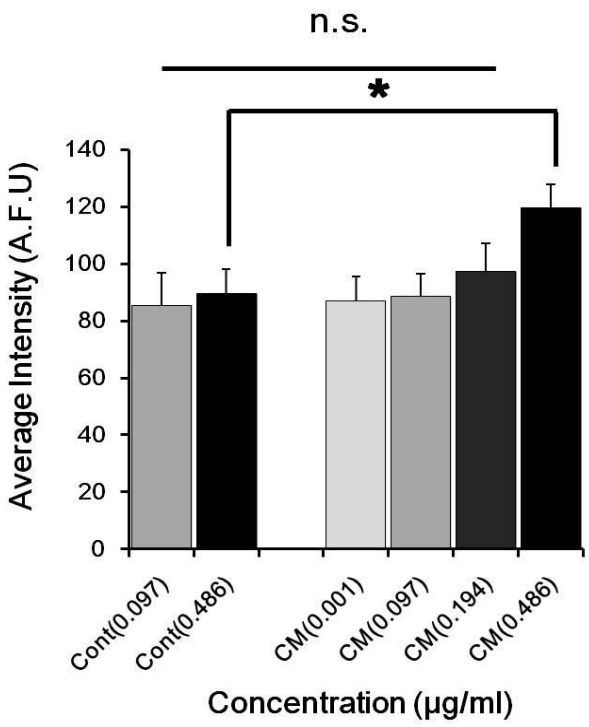

Figure 9. Secreted α-syn acts in a concentration dependent manner (A) Tfn uptake assay was carried out for 10 min at 37˚C with various concentrations of control medium and CM, n = 8 one-way ANOVA followed by the Tukey's HSD *post hoc* test, *p< 0.05

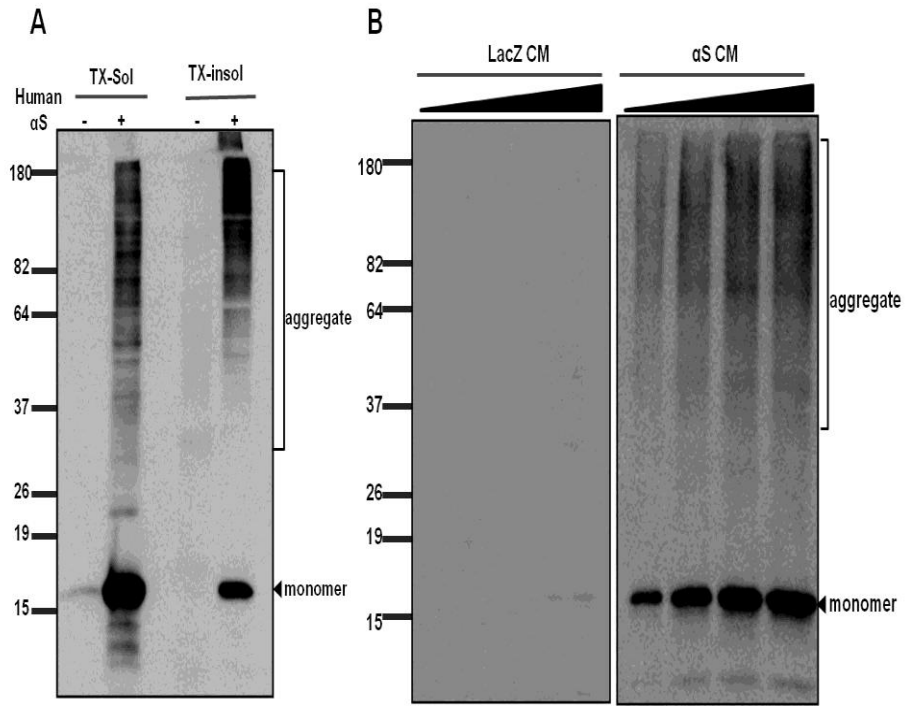

Figure 10. Western blot analysis of α-syn in cell extracts and CM (A) Western analysis of α-syn in the extracts. Differentiated SH-SY5Y cells were infected with adenoviral vector expressing human α-syn. Tx-s, Triton X-100-soluble; Tx-in, Triton X-100-insoluble. **(B)** Western analysis of α-syn in the CM. The levels of α-syn were compared in LacZ CM and α-syn CM.

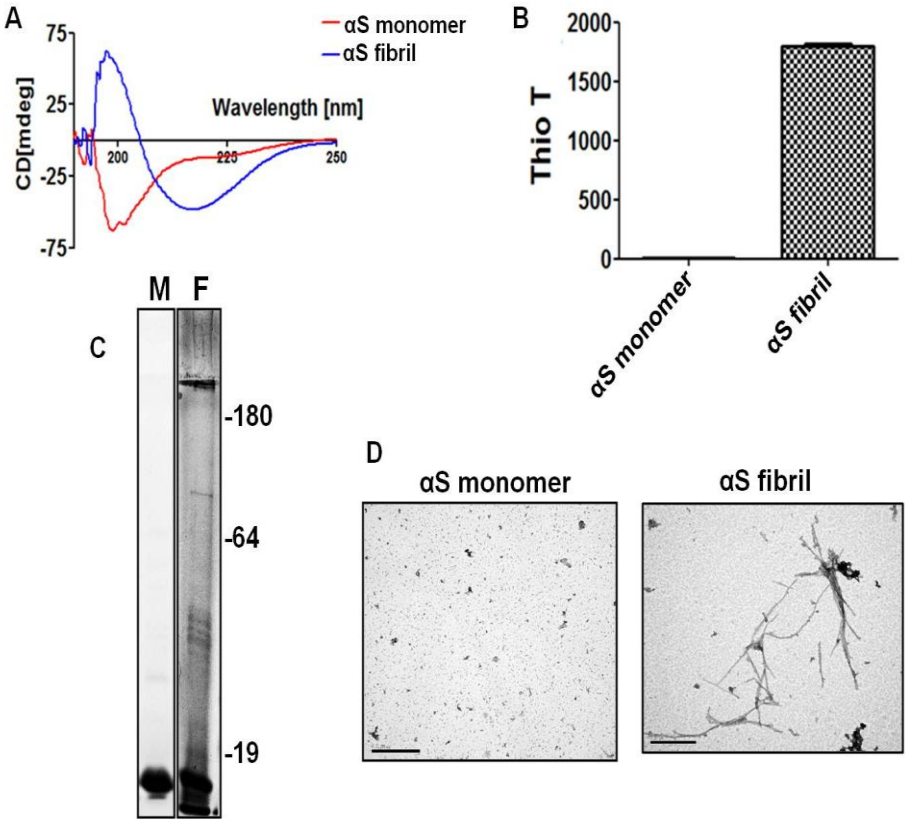

Figure 11. Structural Characterizations of α-synmonomer and fibril (A) Circular dichroism (CD) spectra of α-syn monomer and fibril. Secondary structures of α-syn monomer and fibril (0.5 mg/ml) were analyzed by CD. **(B)** Thioflavin T binding assay Amyloid fibril contents in α-syn monomer and fibril (0.15 mg/ml) were measured by Thioflavin T fluorescence. **(C)** Coomassie staining of α-syn monomer (M) and fibril (F). Coomassie stained fibrils reveal both the SDS-soluble and -insoluble aggregates. Monomer preparation only shows the 15 kD band. **(D)** EM images of α-syn monomer and fibril. Scale bars; 0.5 μm.

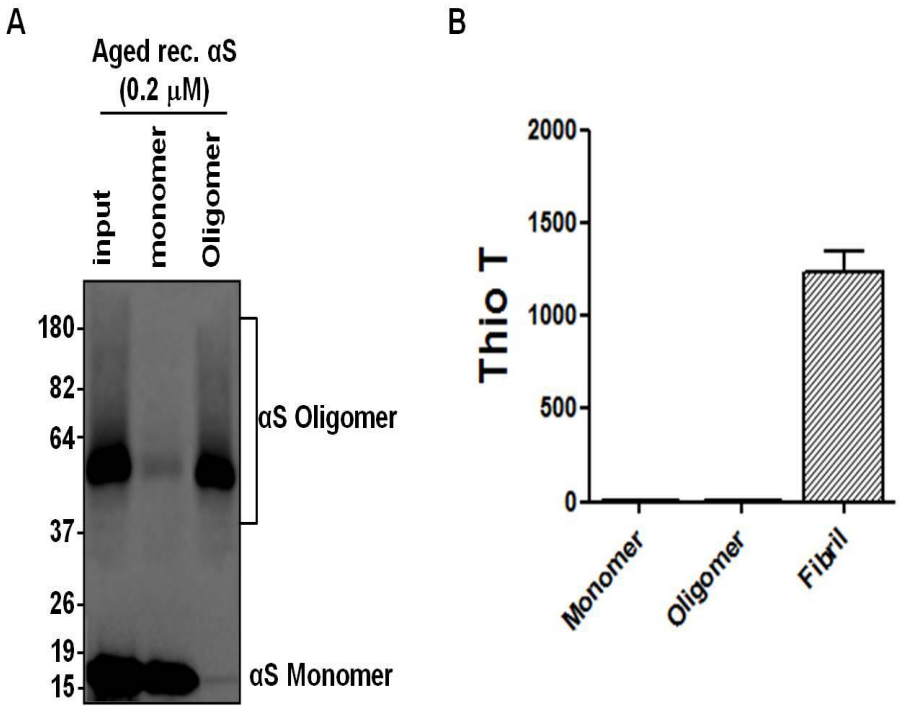

Figure 12. Characterizations of oligomer-containing preparation of α-syn. Two-day-aged recombinant α-syn contains oligomeric and monomeric forms of α-syn. (A) Monomers and oligomers in aged recombinant α-syn were separated by 100,000 molecular weight cut-off filtration. **(B)** Thioflavin T assay of monomeric, oligomeric, and fibril forms of α-syn (10 μM)

DISCUSSION

There is an emerging body of evidence suggesting that α-syn can be secreted in the extracellular space, affecting the homeostasis of recipient cells, possibly by the cell- to-cell transfer mechanism. Recent studies showed that low nanomolar concentrations of monomeric and oligomeric α-syn have been detected in human cerebrospinal fluids (CSF) and blood plasma from PD patients, further emphasizing concerns about the secreted α-syn in the extracellular space (El-Agnaf, Salem et al. 2006; Lee, Lee et al. 2006; Tokuda, Salem et al. 2006).

A few mechanisms such as via exosome or tunneling nanotubes formation have been suggested as to how secreted α-syn transfers between cells (Angot and Brundin 2009; Lee, Desplats et al. 2010) and our results clearly demonstrate that when α-syn is exogenously applied, its uptake is through dynamin-dependent endocytosis rather than other mechanism suggested (**Fig. 1**). The Tfn uptake and release assays have shown that the recycling of Tfn back to the plasma membrane as well as the Tfn internalization is affected by secreted α-syn, indicating that the secreted α-syn induces multiple alterations in membrane trafficking (**Fig. 2 and 3**). Moreover, we show that secreted α-syn enhances the levels of cell surface TfR. Although how endocytosed α-

syn is released into the cytoplasm of the recipient cells remains unsolved (Lee, Desplats et al. 2010), our results suggest that exogenous treatment of secreted α-syn affects various steps in membrane trafficking pathways.

A recent study suggested that the overexpression of α-syn inhibits synaptic vesicle (SV) exocytosis and reduces the recycling fraction of SVs by inhibiting SV reclustering after endocytosis (Nemani, Lu et al. 2010). Our results of α-syn-induced fast endocytosis followed by fast recycling and a high surface resident fraction of TfR seem to be contradictory to their results. Although this may be due to different systems used (COS-7 cells *vs.* cultured neurons), we noticed that they measured the extent of exocytosis but did not test for the kinetics of SV recycling or for the surface resident fraction of SVs (Nemani, Lu et al. 2010). Therefore, we assume that the defects in SV reclustering and reduced recycling fraction of SVs they observed may be due to a high surface fraction of SVs which are less likely to be recycled, which is consistent with our current results on TfR recycling, rather than SV reclustering defect itself although this requires further study.

The central issues associated with secreted α-syn are which species of α-syn are effectively internalized by recipient cells and initiate the intracellular toxic effects. Emmanouilidou *et al.* (2010) and Desplats *et al*. (2009) have

shown that high *n*-oligomeric α-syn in conditioned medium from WT-expressing SH-SY5Y cells can decrease cell viability and exert much greater cytotoxicity in recipient cells compared to the soluble monomeric α-syn (Desplats, Lee et al. 2009; Emmanouilidou, Melachroinou et al. 2010). Park *et al.* (2009) reported that monomeric α-syn was internalized into microglia in a clathrin-, caveolae-, and dynamin-independent manner but, it was dependent on lipid rafts and ganglioside GM1, suggesting that monomeric α-syn was internalized into microglia via another less characterized pathway (Park, Kim et al. 2009). Other studies, however, suggest that monomeric α-syn can directly translocate through the plasma membrane, accounting for the penetration of monomeric α-syn into cells while α–syn forms with higher molecular weight, fibrils and oligomers were internalized through an endocytic pathway (Ahn, Paik et al. 2006; Lee, Suk et al. 2008). Moreover, monomeric α-syn is internalized into neuronal cells in a temperature-independent manner, whereas aggregated α-syn is internalized into the cells by a temperature-dependent endocytosis mechanism, further supporting the idea that secreted α-syn may be internalized by different routes, depending on its assembly state or cell-type-specific mechanisms.

Our current results suggest that accumulation and internalization of the secreted oligomeric species of α-syn, rather than monomeric or fibrillar

forms, effectively induce multiple alterations in membrane trafficking. Elucidating the possible mechanism how secreted oligomeric forms of α-syn are accumulated and may induce multiple alterations in membrane trafficking would be greatly helpful for the development of new therapeutic strategies and the treatment of α-syn-related neuronal degeneration in PD.

REFERENCES

Ahn, K. J., S. R. Paik, et al. (2006). "Amino acid sequence motifs and mechanistic features of the membrane translocation of alpha-synuclein." J Neurochem **97**(1): 265-279.

Angot, E. and P. Brundin (2009). "Dissecting the potential molecular mechanisms underlying alpha-synuclein cell-to-cell transfer in Parkinson's disease." Parkinsonism Relat Disord **15 Suppl 3**: S143-147.

Bae, E. J., H. J. Lee, et al. (2012). "Antibody-aided clearance of extracellular alpha-synuclein prevents cell-to-cell aggregate transmission." J Neurosci **32**(39): 13454-13469.

Ben Gedalya, T., V. Loeb, et al. (2009). "Alpha-synuclein and polyunsaturated fatty acids promote clathrin-mediated endocytosis and synaptic vesicle recycling." Traffic **10**(2): 218-234.

Cheung, A. Y. and S. C. de Vries (2008). "Membrane trafficking: intracellular highways and country roads." Plant Physiol **147**(4): 1451-1453.

Desplats, P., H. J. Lee, et al. (2009). "Inclusion formation and neuronal cell death through neuron-to-neuron transmission of alpha-synuclein." Proc Natl Acad Sci U S A **106**(31): 13010-13015.

Du, J., J. Zhang, et al. (2011). "In vivo RNAi screen reveals neddylation genes as novel regulators of Hedgehog signaling." PLoS One **6**(9): e24168.

El-Agnaf, O. M., S. A. Salem, et al. (2003). "Alpha-synuclein implicated in Parkinson's disease is present in extracellular biological fluids, including human plasma." FASEB J **17**(13): 1945-1947.

El-Agnaf, O. M., S. A. Salem, et al. (2006). "Detection of oligomeric forms of alpha-synuclein protein in human plasma as a potential biomarker for Parkinson's disease." FASEB J **20**(3): 419-425.

Emmanouilidou, E., K. Melachroinou, et al. (2010). "Cell-produced alpha-

synuclein is secreted in a calcium-dependent manner by exosomes and impacts neuronal survival." J Neurosci **30**(20): 6838-6851.

Hansen, C., E. Angot, et al. (2011). "alpha-Synuclein propagates from mouse brain to grafted dopaminergic neurons and seeds aggregation in cultured human cells." J Clin Invest **121**(2): 715-725.

Hansen, C. and J. Y. Li (2012). "Beyond alpha-synuclein transfer: pathology propagation in Parkinson's disease." Trends Mol Med **18**(5): 248-255.

Jang, A., H. J. Lee, et al. (2010). "Non-classical exocytosis of alpha-synuclein is sensitive to folding states and promoted under stress conditions." J Neurochem **113**(5): 1263-1274.

Kim, S., H. Kim, et al. (2006). "Regulation of transferrin recycling kinetics by PtdIns[4,5]P2 availability." FASEB J **20**(13): 2399-2401.

Kim, Y., J. Park, et al. (2010). "Overexpression of Dyrk1A causes the defects in synaptic vesicle endocytosis." Neurosignals **18**(3): 164-172.

Lee, H. J., E. J. Bae, et al. (2011). "Enzyme-linked immunosorbent assays for alpha-synuclein with species and multimeric state specificities." J Neurosci Methods **199**(2): 249-257.

Lee, H. J., S. Patel, et al. (2005). "Intravesicular localization and exocytosis of alpha-synuclein and its aggregates." J Neurosci **25**(25): 6016-6024.

Lee, H. J., J. E. Suk, et al. (2008). "Assembly-dependent endocytosis and clearance of extracellular alpha-synuclein." Int J Biochem Cell Biol **40**(9): 1835-1849.

Lee, P. H., G. Lee, et al. (2006). "The plasma alpha-synuclein levels in patients with Parkinson's disease and multiple system atrophy." J Neural Transm **113**(10): 1435-1439.

Lee, S., K. Y. Jung, et al. (2010). "Synthesis of potent chemical inhibitors of dynamin GTPase." Bioorg Med Chem Lett **20**(16): 4858-4864.

Lee, S. J., P. Desplats, et al. (2010). "Cell-to-cell transmission of non-prion protein aggregates." Nat Rev Neurol **6**(12): 702-706.

Matsui, T., T. Itoh, et al. (2011). "Small GTPase Rab12 regulates constitutive degradation of transferrin receptor." Traffic **12**(10): 1432-1443.

Nemani, V. M., W. Lu, et al. (2010). "Increased expression of alpha-synuclein reduces neurotransmitter release by inhibiting synaptic vesicle reclustering after endocytosis." Neuron **65**(1): 66-79.

Park, J., Y. Kim, et al. (2010). "SNX18 shares a redundant role with SNX9 and modulates endocytic trafficking at the plasma membrane." J Cell Sci **123**(Pt 10): 1742-1750.

Park, J. Y., K. S. Kim, et al. (2009). "On the mechanism of internalization of alpha-synuclein into microglia: roles of ganglioside GM1 and lipid raft." J Neurochem **110**(1): 400-411.

Reynolds, N. P., A. Soragni, et al. (2011). "Mechanism of membrane interaction and disruption by alpha-synuclein." J Am Chem Soc **133**(48): 19366-19375.

Tokuda, T., S. A. Salem, et al. (2006). "Decreased alpha-synuclein in cerebrospinal fluid of aged individuals and subjects with Parkinson's disease." Biochem Biophys Res Commun **349**(1): 162-166.

Ullrich, O., S. Reinsch, et al. (1996). "Rab11 regulates recycling through the pericentriolar recycling endosome." J Cell Biol **135**(4): 913-924.

Varkey, J., J. M. Isas, et al. (2010). "Membrane curvature induction and tubulation are common features of synucleins and apolipoproteins." J Biol Chem **285**(42): 32486-32493.

Vekrellis, K., M. Xilouri, et al. (2011). "Pathological roles of alpha-synuclein in neurological disorders." Lancet Neurol **10**(11): 1015-1025.

Volpicelli-Daley, L. A., K. C. Luk, et al. (2011). "Exogenous alpha-synuclein fibrils induce Lewy body pathology leading to synaptic dysfunction and neuron death." Neuron **72**(1): 57-71.

Windisch, M., H. Wolf, et al. (2008). "The role of alpha-synuclein in neurodegenerative diseases: a potential target for new treatment strategies?" Neurodegener Dis **5**(3-4): 218-221.

국문 초록

α-Synuclein 은 뉴런에서 세포 바깥으로 분비 되는데 이는 주변의 셀들의 항상성에 영향을 미치는 것으로 알려졌다. 하지만, 분비된 알파시뉴클린의 병태생리학적 영향은 아직까지 정확하게 알려진바 없다. 본 연구에서는, COS-7 셀 외부에 differentiated SH-SY5Y 셀에서 분비된 알파시뉴클린을 처리하여서 보았을때, 알파시뉴클린은 dynamin 에 의한 endocytosis 를 통해 세포 막 안으로 들어간다는 것을 발견하였다. 또한, 안으로 들어간 알파시뉴클린은 transferrin receptor internalization 그리고, recycling 의 속도에 크게 영향을 미치는 것을 발견할수 있었다. 이러한 영향들은 세포막에 transferrin receptor 의 양을 증가 시켰다. 본연구에서 찾은 영향들은 알파시뉴클린의 monomer 혹은 fibril 형태 보다는 oligomer 형태로서 영향을 미치는 것을 알수 있었다. 이를 통해, 우리는 분비된 알파시뉴클린이 세포막 수송과정의 여러 과정에 문제를 이르키며 이는 파킨슨병의 기초단계의 기능 장애를 일으킬수 있음을 증명하였다.

주요어 : 알파시뉴클린, 파킨슨병, transferrin receptor, 세포막 수송과정, endocytosis

학 번 : 2011-23810